ELSEVIER

Modelling microwave heating

James M. Hill and Timothy R. Marchant

Department of Mathematics, University of Wollongong, Wollongong, New South Wales, Australia

Although microwave radiation is best known for heating food in the kitchen, in recent years it has found new applications in many industrial processes, such as those involving melting, smelting, sintering, drying, and joining. Heating by microwave radiation constitutes a highly coupled nonlinear problem giving rise to new and unexpected physical behavior, the best known of which is the appearance of "hot spots." That is, in many industrial applications of microwave heating it has been observed that heating does not take place uniformly but rather regions of very high temperature tend to form. In order to predict the occurrence of such phenomena it is necessary to develop simplified mathematical models from which insight might be gleaned into an inherently complex physical process. The purpose of this paper is to review some of the recent developments in the mathematical modelling of microwave heating, including models that consider in isolation the heat equation with a nonlinear source term, in which case the electric-field amplitude is assumed constant, models involving the coupling between the electric-field amplitude and temperature including both steady-state solutions and the initial heating, and also models that control the process of thermal runaway. Numerical modelling of the microwave heating process is also briefly reviewed.

Keywords: microwave heating, model equations, Maxwell's equations of electromagnetism, hot spots, low electrical conductivity, forced heat equation, thermal runaway, damped wave equation

1. Introduction

Although the familiar domestic microwave oven has been in use for nearly 50 years, use of this technology for industrial heating applications is a recent development and the bulk of the theoretical work in this area has been undertaken only in the past few years. The present interest in industrial applications of heating by microwave radiation, such as in melting, smelting, sintering, drying, and joining, has prompted a good deal of research that aims to formulate mathematical models capable of accurately modelling the phenomena. In general a proper study of microwave heating involves solving Maxwell's equations of electromagnetism and the forced heat equation where all thermal, electrical, and magnetic properties of the material are nonlinearly dependent on the temperature T. In the full mathematical problem, Maxwell's equations and the forced heat equation are coupled and grossly nonlinear and this depth of complexity is revealed in applications through the appearance of unusual and often unexpected physical behavior such as "hot spots" and "waiting time" phenomena. Hot spots occur in a material irradiated by microwaves due to the temperature-dependent material properties. The rate of absorption of microwave energy referred to as the thermal absorptivity usually increases with temperature, hence thermal runaway can result. The location of a hot spot in the material arises from differential heating and can be due to a small temperature anomaly, an impurity of higher thermal absorptivity, or simply to a geometrical feature such as a corner or edge. In addition some materials are transparent to microwave radiation and yet after heating by conventional means they respond to microwave energy. Similarly, waiting-time behavior is exhibited by materials that respond to microwave heating only after a finite amount of time has elapsed. In this paper we review recent mathematical developments in these areas.

To solve fully Maxwell's equations coupled with the forced heat equation, it is necessary to prescribe the temperature-dependent material properties, namely the specific heat, $c(T)$; thermal diffusivity, $\nu(T)$; thermal absorptivity, $\gamma(T)$; magnetic permeability, $\mu(T)$; electrical permittivity, $\epsilon(T)$; and the electrical conductivity, $\sigma(T)$. An accurate experimental determination of these six material parameters over some temperature range constitutes a formidable obstacle, and existing mathematical models of microwave heating emerge according to the assumed knowledge of these electrical, magnetic, and thermal properties.

In Section 2 of this paper, the equations that govern microwave heating are given, namely Maxwell's equations of electromagnetism, which describe the propagation of the electric and magnetic fields, and the forced heat equation, which describes the absorption and diffusion of heat. The usual approximations are made to simplify these equations to obtain the damped wave equation, obtained from Maxwell's equations in the limit of small electrical con-

Address reprint requests to Prof. James M. Hill at the Department of Mathematics, University of Wollongong, Wollongong, NSW 2522, Australia.

Received 29 November 1993; accepted 7 March 1994

Appl. Math. Modelling 1996, Vol. 20, January

655 Avenue of the Americas, New York, NY 10010

0307-904X/96/$15.00
SSDI 0307-904X(95)00107-U

ductivity and slowly varying electrical permittivity and magnetic permeability, and the transport equation, derived from Maxwell's equations in the high-frequency limit. Also presented are the appropriate initial and boundary conditions for the electric field and the temperature.

In Section 3, thin materials are considered so that the assumption of constant electric-field amplitude is made. This assumption simplifies the problem by allowing the forced heat equation to be solved in isolation. Typically, the thermal absorptivity $\gamma(T)$ is assumed to have a given dependence on temperature, and steady-state temperature profiles are found. In regions of parameter space where steady-state solutions do not exist, it is postulated that thermal runaway occurs.

In Section 4, models are considered that incorporate the coupled electric-field amplitude and temperature. Hence, the electric-field amplitude decays through the slab with spatial exponential decay occurring in the case of constant electrical conductivity. Steady-state solutions of this coupled system are found. For some choices of electrical conductivity the power versus temperature curve is S-shaped giving rise to one or three steady-state solutions with a hysteresis effect in the multivalued region. At a certain critical power level, the solution jumps from the lower branch to the upper branch of the S-shaped curve resulting in thermal runaway.

In Section 5, the coupled system of the damped wave equation, valid for small electrical conductivity, and the forced heat equation are considered. Asymptotic solutions obtained by the methods of multiple scales and strained coordinates are reviewed. In Section 6, the dynamics and control of thermal runaway are examined. The input power is assumed to be a function of time, and various control models such as feedback stabilization are considered to enable the appropriate steady-state solution to be achieved. In Section 7, numerical modelling is briefly surveyed, which is important both as a means of verifying analytical solutions and to model problems that are intractable by other means, such as the drying of a porous material using microwave energy.

2. Governing equations

The equations that govern microwave heating of a material are Maxwell's equations, which govern the propagation of the microwave radiation, and the forced heat equation, which governs the absorption and diffusion of heat by the material. If the material is assumed to be homogeneous, isotropic, and Ohmic, that is the current $\underset{\sim}{J}$ and the displacement current $\underset{\sim}{D}$ are both proportional to the electric field $\underset{\sim}{E}$ and that the magnetic flux density $\underset{\sim}{B}$ is proportional to the magnetic field strength $\underset{\sim}{H}$, then Maxwell's equations of electromagnetism are given by[1]

$$\nabla\cdot\underset{\sim}{D}=\nabla\cdot(\epsilon\underset{\sim}{E})=\rho \qquad \nabla\cdot\underset{\sim}{B}=\nabla\cdot(\mu\underset{\sim}{H})=0$$
$$\nabla\times\underset{\sim}{E}=-\frac{\partial}{\partial t}(\mu\underset{\sim}{H}) \qquad \nabla\times\underset{\sim}{H}=\frac{\partial}{\partial t}(\epsilon\underset{\sim}{E})+\sigma\underset{\sim}{E} \tag{1}$$

where σ is the electrical conductivity, ϵ is the electrical permittivity, and μ is the magnetic permeability. In general, all the material properties are temperature-dependent. For a plane wave propagating in the positive x-direction, it can be assumed, without loss of generality, that the electric field is in the y-direction and the magnetic field is in the z-direction. Thus for the heating of a one-dimensional body, the electric and magnetic fields are functions of the spatial co-ordinate x and time t only. If the net free charge ρ is zero, then Maxwell's equations reduce to

$$E_x=-(\mu H)_t \qquad H_x=-(\epsilon E)_t-\sigma E \tag{2}$$

Since equation (2) is temperature-dependent, it is coupled with the forced heat equation

$$\rho c_p(T)T_t=[\nu(T)T_x]_x+\gamma(T)\,|E|^2 \tag{3}$$

where ν is the thermal diffusivity, γ is the thermal absorptivity, ρ is the density that is usually assumed constant, and c_p is the specific heat. The thermal absorptivity evidently depends on the square of the electric-field amplitude and it is assumed that the heating occurs on a length scale much greater than a microwave length, so that in equation (3) the absorption of heat is averaged over a wavelength. Alternatively, equation (3) can be obtained by assuming that the time taken for heat to diffuse a microwave length is much greater than the period of the microwave radiation.[2]

In general, Maxwell's nonlinear equations are intractable, and various simplifying assumptions are necessary to obtain analytical mathematical solutions. If the electrical permittivity and the magnetic permeability are assumed to both be slowly varying functions of the temperature, and the electrical conductivity is assumed to be small, then Pincombe and Smyth[3] show that equation (2) can be reduced to the damped wave equation

$$E_{tt}+AE_t=c^2E_{xx}$$
$$A=\mu_t/\mu+2\epsilon_t/\epsilon+\sigma/\epsilon-c\mu_x/\mu \tag{4a–b}$$

and μ, ϵ, and $c=(\mu\epsilon)^{-\frac{1}{2}}$ are slowly varying and σ is small. In addition if c_p and ν are taken to be constant then the forced heat equation can be written in the form

$$T_t=\nu T_{xx}+\gamma(T)\,|E|^2 \tag{5}$$

and the combination of this equation and the damped wave equation (4) is considerably, more amenable to analytical techniques. Initially we suppose that no microwave radiation is present in the material and that for a semi-infinite slab ($x>0$) microwave radiation

$$E=E_i[e^{i(k_v x-\omega t)}+re^{-i(k_v x+\omega t)}] \qquad x<0 \tag{6}$$

of constant amplitude E_i, frequency ω, and wavenumber k_v in free space is incident upon the slab. A portion of the radiation with amplitude r is reflected at the material boundary while the remainder of the radiation is transmitted into the material. The electric field and its derivative are continuous at the boundary ($x=0$) and initially there is no radiation present in the material so that we have the boundary and initial conditions

$$E_x(0, t) + ik_v E(0, t) = 2ik_v E_i e^{-i\omega t}$$
$$E(x, 0) = 0 \tag{7}$$

where $c_v = \omega/k_v$ is the velocity of the radiation in free space. For a finite slab (with the rear edge at $x = h$) this is supplemented with the additional boundary condition

$$E_x(h, t) - ik_v E(h, t) = 0 \tag{8}$$

which ensures that the electric field and its derivative are also continuous at the rear edge of the slab. The appropriate initial and boundary conditions for the temperature T are

$$T = T_i \text{ on } t = 0$$
$$T_x - B_i(T - T_i) - B_r(T^4 - T_i^4) = 0 \text{ on } x = 0$$
$$T_x + B_i(T - T_i) + B_r(T^4 - T_i^4) = 0 \text{ on } x = h \tag{9a–c}$$

where B_i is the Biot number, which is a measure of the convective heat loss, and B_r is the radiation equivalent of the Biot number. In the small convective and radiative heat-loss limit (B_i, $B_r \to 0$), the zero heat-flux boundary condition applies. In the large radiative and convective heat-loss limit (B_i, $B_r \to \infty$), heat loss from the material is significant and a fixed-temperature boundary condition applies. The fixed-temperature boundary condition is a good approximation for dielectric materials since the Biot-number and its radiation equivalent are small (for example, $B_i \sim 10^{-4}$ for ceramics[4]). Initially the material is assumed to be at a uniform temperature T_i (equation [9a]).

A further simplification can be made by assuming that the frequency of the radiation is large ($\omega \gg 1$). The high-frequency assumption means that the wavelength of the radiation is very small compared with a typical body dimension of the material being heated which in the case of a semi-infinite body could be taken as the distance the wavefront has travelled. It is also implicitly assumed that the other parameters are all of order one. In particular, this implies $\omega \gg \sigma$ and the high-frequency assumption is equivalent to assuming small electrical conductivity.[3] A geometric optics (WKB) expansion is performed by assuming the form

$$E = \phi(x, t)e^{i\omega\theta} + \omega^{-1}\phi_1(x, t)e^{i\omega\theta} + \dots$$
$$\omega \gg 1 \tag{10}$$

where the phase function θ represents the fast oscillations of the wavetrain, while the amplitude terms ϕ and ϕ_1 are modulated by slow variations only since the wavetrain properties vary slowly over the scale of an extremely small wavelength. The expansion (10) is substituted into the damped wave equation (4) and expanded in powers of ω. At order ω^2 the eikonal equation is obtained

$$\theta_t + c\theta_x = 0 \tag{11}$$

which shows that the wavetrain travels at speed c. At order ω the transport equation

$$2\phi_t\theta_t + \theta_{tt}\phi + A\theta_t - \phi_1\theta_t^2$$
$$= c^2(2\phi_x\theta_x + \phi\theta_{xx} - \phi_1\theta_x^2) \tag{12}$$

is obtained. Using equation (11) in (12) gives the transport equation in the form

$$\phi_t + c\phi_x = -\frac{\phi}{2}[A - c_x + c_t/c] \tag{13}$$

which is the equation that governs the modulation of the leading order amplitude ϕ. Equation (13) can also be obtained directly by substituting equation (10) and an equivalent expression for the magnetic field strength $\underset{\sim}{H}$ into Maxwell's equations (2).[5] Equation (13) is also identical to equation (3.8) of Pincombe and Smyth,[3] which is derived under the assumption of small electrical conductivity and slowly varying electrical permittivity and magnetic permeability.

In some work, the forced heat equation is considered in the limit of no diffusion ($\nu = 0$) so that equation (5) becomes

$$T_t = \gamma\,|\,\phi\,|^2 \tag{14}$$

and this assumption is valid when the time scale for microwave heating is small compared with the time scale over which the diffusion of heat occurs. For example, for certain ceramics the scaled diffusivity $\nu = 1 \times 10^{-9}$ (see Marchant and Smyth[6]).

Maxwell's equations (2) and the general forced heat equation (3) also admit travelling wave solutions of the form

$$T = f(\xi) \qquad E = g(\xi) \qquad H = h(\xi) \tag{15}$$

where $\xi = \alpha x + \beta t$ and α and β denote arbitrary constants. We observe that such special solutions may be valuable as a means of checking numerical schemes and also include time independent and spatially independent solutions as special cases arising from $\beta = 0$ and $\alpha = 0$, respectively. Further special solutions of the full coupled system of equations (2) and (3) can be obtained by assuming certain special forms of the material parameters. Metaxas and Meredith[7] present experimental evidence that indicates that the thermal, electric, and magnetic properties of certain materials have a power-law dependence on temperature. Assuming that the various properties of the material all take the form

$$\Phi(T) = \Phi_0(T - T_0)^m \tag{16}$$

for various constants m and Φ_0 but where T_0 is assumed to be the same reference temperature for each property, then it is possible to deduce further special solutions of equations (2) and (3) such as stretching similarity solutions of the form

$$T = x^b f(\xi) \qquad E = x^c g(\xi) \qquad H = x^d h(\xi) \tag{17}$$

where $\xi = x^a/t$ and a, b, c, and d denote certain constants, or special separable solutions such as

$$T = t^A f(x) \qquad E = t^B g(x) \qquad H = t^C h(x) \tag{18}$$

for certain constants A, B and C.[8] In all the above solutions, f, g, and h refer to arbitrary functions of the indicated argument which are determined by solving three ordinary highly nonlinear differential equations. Even if these equations can be integrated, the available solutions are limited to the above special forms and generally we may expect that further analytical results can only be achieved by major simplifications of the coupled system in equations (2) and (3).

3. Nonlinear heat model and hot spots

In view of the practical difficulty in determinating the six physical properties of the material over some temperature range, the prospect of replacing the full coupled system (1) and (3) simply with a heat equation that incorporates a nonlinear thermal absorptivity is an extremely attractive one. Assuming constant specific heat and that the thermal conductivity and electrical-field amplitude are constant, the appropriate form of equation (3) generalized to three dimensions becomes

$$\frac{\partial T}{\partial t} = \nabla^2 T + \gamma(T) \tag{19}$$

where ∇^2 is the usual Laplacian operator and we assume that the length and time scales have been suitably nondimensionalized. In a recent article appearing in this journal, Hill and Jennings[9] undertake an exhaustive investigation of the experimental results of Von Hippel[10] to determine as accurately as possible the precise nature of the thermal absorptivity $\gamma(T)$. The form of $\gamma(T)$ depends upon the material under consideration, the temperature range under investigation, and the frequency of the microwave radiation. At higher frequencies (10^{10} Hz) materials such as fused silica glass are very accurately approximated by quadratic and linear functions for $\gamma(T)$, namely

$$\gamma(T) = A + BT + CT^2 \qquad \gamma(T) = A + BT \tag{20}$$

for certain constants A, B, and C. We remark that in these cases the close agreement with experimental results is quite striking. At lower frequencies (10^7 Hz), $\gamma(T)$ can be adequately approximated by one of the exponential forms

$$\gamma(T) = Ae^{\alpha T} \qquad \gamma(T) = Be^{-\beta(T-T_0)^2} \tag{21}$$

where A, B, T_0, α, and β denote constants and both provide almost the same level of agreement with experimental results which is not as good as the agreement obtained for the higher frequencies. At even lower frequencies (10^2–10^4 Hz) the experimental results of Von Hippel[10] can be quite accurately approximated by a linear combination of the exponential in equation (21), namely

$$\gamma(T) = Ae^{\alpha T} + Be^{-\beta(T-T_0)^2} \tag{22}$$

Figure 1 shows the thermal absorptivity $\gamma(T)$ versus T for Mycalex 2021, which is a form of mica, at 10^4 Hz. The figure shows both the experimental data and the fitted curve (22). The initial portion of the curve shown in *Figure 1* is the exponential growth previously described, while the variation in $\gamma(T)$ about the minimum is accurately approximated by a quadratic, indicating that the forms obtained at the higher frequencies are embodied in the general picture described by equation (22).

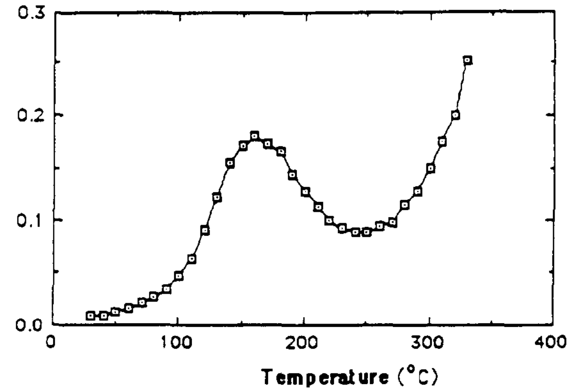

Figure 1. Thermal absorptivity $\gamma(T)$ versus T for Mycalex 2021 at 10^4 Hz.

Even though, at first sight equation (19) appears to be a very naive approximation to the full coupled system, we can immediately recognize its relevance to the theory of hot spots in the following manner. In this phenomena, a localized temperature anomaly is magnified out of all proportion. For example, bricks undergoing microwave drying often explode due to the formation of hot spots. As a first approximation for a body with initial uniform temperature, we might assume that spatial variations in temperature are negligible and accordingly replace equation (19) by

$$\frac{dT}{dt} = \gamma(T) \tag{23}$$

which is a reasonable first approximation for most microwave applications, because the heating is so rapid that there is neglibible heat loss through the surface of the body. For example, in the case of exponential thermal absorptivity $\gamma(T) = \gamma_0 e^T$, the solution to equation (23) is the spatially uniform temperature field

$$T_1(t) = -\log(1 - \gamma_0 t) \tag{24}$$

where initially the material is of zero temperature. Solution (24) clearly "blows-up" in finite time $t_f = \gamma_0^{-1}$. The same property holds for any $\gamma(T)$, which grows faster than a linear thermal absorptivity.[11] Coleman[11] postulates that the phenomenon of hot spots is due to the existence of thermal instabilities and he examines the conditions under which a spatially uniform temperature field $T_1(t)$ is unstable. For a small perturbation from this temperature distribution, namely

$$T(\underset{\sim}{r}, t) = T_1(t) + u(\underset{\sim}{r}, t) \tag{25}$$

we find from equation (19) that

$$\frac{\partial u}{\partial t} = \nabla^2 u + \gamma'(T_1)u \tag{26}$$

where the prime here denotes differentiation with respect to T_1. Equation (26) has a separable solution for $u(\underset{\sim}{r}, t)$ of the form

$$u(\underset{\sim}{r}, t) = f(\underset{\sim}{r})\gamma[T_1(t)]e^{-\lambda t} \tag{27}$$

where λ denotes the separation constant and $f(\underset{\sim}{r})$ satisfies the Helmholtz equation

$$\nabla^2 f + \lambda f = 0 \tag{28}$$

Now the spatially uniform temperature distribution $T_1(t)$ is unstable in finite time if $u(\underset{\sim}{r}, t)/T_1(t)$ tends to infinity in finite time, which will certainly be the case for equation (27) provided

$$\gamma(T_1)/T_1 \to \infty \text{ as } t \to t_f \tag{29}$$

where t_f designates some finite time. Of particular relevance in the short term is whether or not the normalized perturbation $u(\underset{\sim}{r}, t)/T_1(t)$ will peak, and from equation (27) and the condition

$$\frac{\partial}{\partial t}\left[\frac{u(\underset{\sim}{r}, t)}{T_1(t)}\right] = 0 \tag{30}$$

we may deduce

$$\gamma'(T_1) = \lambda + \gamma(T_1)/T_1 \tag{31}$$

Coleman[11] demonstrates that in the case of the Arrhenius law $\gamma(T) = \gamma_0 e^{-1/T}$ the roots of equation (31) cease to exist for λ/γ_0 above a value of about 0.305 and therefore the ratio λ/γ_0 needs to be as large as possible for the peak to be eliminated, or at least moderated.

Alternatively, if a finite material of initially uniform temperature subject to fixed temperature boundary conditions ($T = T_1$) is considered, then Hill and Smyth[12] postulate that a hot spot occurs when a steady-state solution of the forced heat equation ([19] with $T_t = 0$) does not exist. In particular for exponential $\gamma(T) = \gamma_0 e^T$, the problems for a slab of length two and for a cylinder of unit radius are described by

$$\frac{d^2T}{dx^2} + \gamma_0 e^T = 0 \quad \frac{dT}{dx}(0) = 0 \quad T(\pm 1) = T_1$$

$$\frac{d^2T}{dr^2} + \frac{1}{r}\frac{dT}{dr} + \gamma_0 e^T = 0 \quad \frac{dT}{dr}(0) = 0 \tag{32}$$

$$T(1) = T_1$$

Equations (32) have well known exact solutions,

$$T(x) = T_0 - 2\log_e \cosh\left(\frac{\gamma_0 e^{T_0}}{2}\right)^{1/2} x$$

$$T(r) = T_0 - 2\log_e\left(1 + \frac{\gamma_0 e^{T_0} r^2}{8}\right) \tag{33a–b}$$

respectively, where in each case T_0, the temperature in the center, is determined from the transcendental equation arising from the fixed-temperature boundary condition $T(1) = T_1$. If the stability condition

$$T_1 < \log_e(2/\gamma_0 \kappa_0^2) \tag{34}$$

is satisfied where κ_0 is a number given by

$\kappa_0 = 1.5089(\text{planar}) \qquad \kappa_0 = 1.0(\text{cylinder})$

$\kappa_0 = 0.786(\text{sphere})$

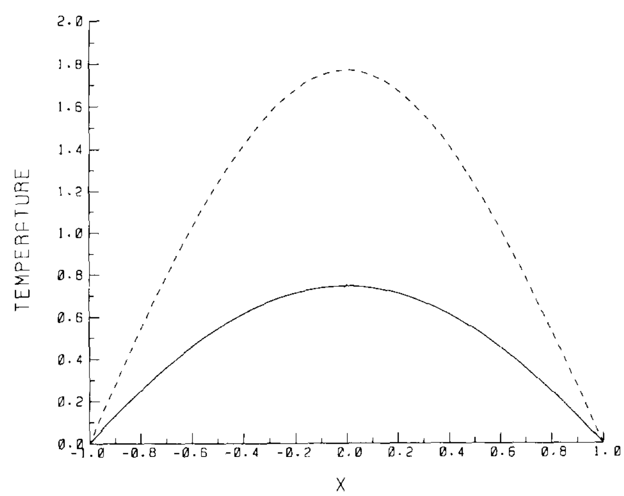

Figure 2. The temperature T versus x for $\gamma_0 = 0.8$, $T_1 = 0$, and $t = 10$. Shown are the two steady-state temperature profiles (33a) and the numerical solution to equation (5) (———).

then two steady-state temperature profiles exist. If equation (34) is not satisfied then thermal runaway occurs resulting in a hot spot. In the planar and cylindrical geometries the steady-state solutions are given by equations (33), while in the case of a sphere of unit radius an explicit analytical solution cannot be found and the stability condition (34) is found numerically. *Figure 2* shows the slab temperature T versus x for $\gamma_0 = 0.8$, $T_1 = 0$, and $t = 10$. Two steady-state temperature profiles are shown, obtained directly from equation (33), and the numerical solution to (5)(———) is also shown. We observe that the agreement between the lower steady-state solution and the numerical solution is excellent. This confirms the stability analysis performed by Hill and Smyth,[12] which suggests that the lower temperature profile is the stable one while the higher temperature profile is unstable.

Roussy et al.[13] adopt a similar approach for a cylindrical sample, assuming a quadratic thermal absorptivity. Assuming constant specific heat and thermal conductivity, they examine numerically the conditions under which the solution of

$$\frac{\partial T}{\partial t} = \left(\frac{\partial^2 T}{\partial r^2} + \frac{1}{r}\frac{\partial T}{\partial r}\right) + \gamma_0\left[1 + \gamma_1\left(\frac{T - T_0}{T_0}\right) + \gamma_2\left(\frac{T - T_0}{T_0}\right)^2\right] \tag{35}$$

subject to the initial and boundary conditions comprising an initial uniform temperature (9a) and the convective heat-loss boundary condition applied at $r = a$ ([9c] with $B_r = 0$). On introducing the new variables and the function $R(\alpha, \beta, \gamma_1, \gamma_2)$ defined by

$$\alpha = \frac{2T_0}{a^2\gamma_0} \qquad \beta = \frac{2B_i T_0}{a\gamma_0}$$

$$R(\alpha, \beta, \gamma_1, \gamma_2) = \frac{\beta^2}{\gamma_1^2 + 4\gamma_2}\left(1 - \frac{\gamma_2}{3\alpha^2}\right) \tag{36}$$

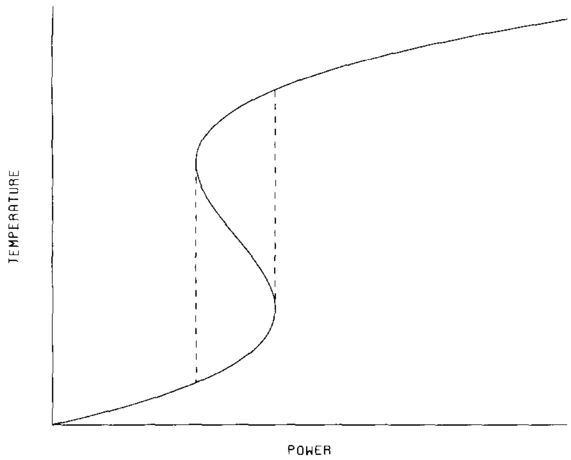

Figure 3. A typical S-shaped power versus temperature profile. The dashed lines are drawn at the critical power levels.

the authors make the fascinating speculation, based on numerical evidence, that thermal runaway occurs when $R < 1$ while the solution of equation (25) is stable for $R > 1$. Brodwin et al.[14] found steady-state solutions of equation (19) with thermal absorptivity, $\gamma(T) = \gamma_0 e^{\gamma_1 T}$, with convective and radiative heat-loss boundary conditions ([9b] and [9c]). They found that the steady-state temperature as a function of incident microwave power is an S-shaped curve. *Figure 3* shows a typical S-shaped power versus temperature curve. It can be seen that the temperature is a multivalued function of the power. The upper and lower branches of the curve are stable, while the middle branch is unstable and the hystersis effect is generated as follows. As the power increases from zero, the steady-state solution stays on the lower branch until a certain critical power; then an infinitesimal increase in power will cause the steady-state solution to jump to the upper branch. This temperature jump is indicated by the dashed line on the right and represents thermal runaway. If the power is now decreased, the steady-state solution will stay on the upper branch until reaching the second critical power level where the steady-state solution jumps back to the lower branch, and this temperature decrease is indicated by the dashed line on the left and represents thermal rundown.

4. Models incorporating the electric field

In an attempt to provide a more realistic model of microwave heating, we retain the nonlinear heat equation (5) but assume that the electric-field amplitude decays exponentially with distance, that is we assume

$$|E| = E_0 e^{-\kappa x} \qquad (37)$$

where E_0 is the amplitude of the incident radiation and κ is the decay rate. This assumption is made because first it is a well known result in the case when the permeability, permittivity and electrical conductivity are known to be constants, say μ_0, ϵ_0, and σ_0, respectively, in which case the decay constant κ is given by

$$\kappa = \omega\left(\frac{\mu_0\epsilon_0}{2}\right)^{1/2}\left[\left(1+\left(\frac{\sigma_0}{\epsilon_0\omega}\right)^2\right)^{1/2} - 1\right]^{1/2} \qquad (38)$$

where ω denotes the frequency of the microwave radiation.[7] Second, the assumption in equation (37) will be locally valid within a limited region, depending on the variation of $\mu(T)$, $\epsilon(T)$, and $\sigma(T)$. Finally the assumption in (37) pertains to the electric-field amplitude rather than the electric field itself, so that provided $E(x, t)$ takes the form

$$E(x, t) = E_0 e^{-\kappa x} e^{i\Theta(x,t)} \qquad (39)$$

for some real phase function $\Theta(x, t)$, assumption (37) remains valid. Thus equation (37) represents the simplest possible spatial dependence which has some accepted physical basis but which still enables the heating aspects of the problem to be isolated from the electric and magnetic fields.

Hill and Pincombe[15] consider similarity solutions for two basic models, the first based on power-law thermal properties and the second based on exponential thermal properties, namely

$$\frac{\partial T}{\partial t} = \frac{\partial}{\partial x}\left(T^m \frac{\partial T}{\partial x}\right) + \alpha e^{-\beta x} T^n$$
$$\frac{\partial T}{\partial t} = \frac{\partial}{\partial x}\left(e^{\gamma T} \frac{\partial T}{\partial x}\right) + \alpha e^{-\beta x} e^{\delta T} \qquad (40a\text{–}b)$$

where the constants α, β, n, m, γ, and δ are assumed positive. In particular for the first model, Hill and Pincombe[15] examine in detail the following similarity temperature profiles:

$$T(x, t) = e^{-x/ma}\phi(\xi) \qquad \xi = te^{-x/a}$$
$$a = \frac{(m+1-n)}{\beta m} \qquad (m \neq 0,\ n \neq m+1)$$
$$T(x, t) = t^{-1/m}\phi(x) \qquad (m \neq 0,\ n = m+1)$$
$$(41a\text{–}c)$$
$$T(x, t) = e^{-ax}\phi(x - bt) \qquad a = \frac{\beta}{(1-n)}$$
$$(m = 0,\ n \neq 1,\ b \text{ arbitrary})$$

where in each case the function ϕ is determined by substitution into equation (40a). A particularly simple special case of the last solution ($b = 0$) is

$$T(x, t) = e^{-ax}\left(Ce^{(1-n)a^2 t} - \frac{\alpha}{a^2}\right)^{1/(1-n)} \qquad (42)$$

where a is as previously defined and C denotes an arbitrary constant of integration. If $n > 1$ and $\beta > 0$ then $a < 0$ and blow-up occurs after a finite time t_f given by

$$t_f = \frac{1}{(n-1)a^2}\log_e\left(\frac{Ca^2}{\alpha}\right) \qquad (43)$$

provided the constant C is such that $C > \alpha/a^2$. For the second model, Hill and Pincombe[15] consider the following similarity profiles:

$$T(x,t) = \frac{bx}{a} + \phi(\xi) \qquad \xi = te^{-x/a}$$
$$a = \frac{(\gamma-\delta)}{\beta\gamma} \qquad b = -\frac{1}{\gamma} \qquad (\gamma \neq 0,\ \delta \neq \gamma)$$
$$T(x,t) = -\frac{\log_e t}{\gamma} + \phi(x) \qquad (\gamma \neq 0,\ \delta = \gamma)$$
$$(44)$$
$$T(x,t) = \frac{1}{\delta}\left[\beta x - 2\log_e(x+x_0) + \phi\left(\frac{x+x_0}{(t+t_0)^{1/2}}\right)\right]$$
$$(\gamma = 0,\ \delta \neq 0,\ t_0 \text{ arbitrary})$$

and again the functions ϕ are determined by substitution into equation (40b) and solving the resulting ordinary differential equation numerically. *Figure 4* shows the solution to equation (41a) for $m = 1$, $n = 3$, $\beta = 1$, and $t = 10$ and $\alpha = 0.5$ (A), $\alpha = 1$ (B), and $\alpha = 2$ (C). *Figure 4a* shows the variable ϕ and *Figure 4b* shows the temperature T. Both the variable ϕ and the temperature profiles show the moving thermal front, which over time moves into the region of zero temperature. This solution is entirely consistent with the observed characteristics of microwave heating. For the second model, moving fronts are also predicted but in this case $T = 0$ is not a valid trivial solution of the equation and therefore the model does not admit the possibility that certain materials can be transparent to microwave radiation.

Using the notion of a hot spot formulated by Hill and Smyth,[12] Smyth[16] utilizes the first power-law model with $m = -1$ to examine the effect of electrical conductivity on hot spot formation. It is shown that the electrical conductivity of the material can have a significant effect and if large enough can stop a hot spot from forming altogether. This is because the electrical conductivity causes the microwave radiation to decay as it propagates through the material, and for large enough values of the electrical conductivity hot spots cannot form. The dependence of the critical value of the thermal conductivity on the other physical parameters of the problem is also determined.

Coleman[17] utilizes the forced heat equation (5) to investigate the microwave heating of a frozen half-space which is an idealization that might provide useful information about the initial stages of heating in more complex geometries. The problem is considered in terms of the low diffusivity limit of the classical Stefan problem, which exhibits superheating, and an alternative formulation based on the enthalpy method is adopted. This indicates that the superheated region should be replaced by a "mushy zone" containing a mixture of phases. The effects of moderate diffusivity and convective heating are investigated since many modern microwave ovens employ both microwave and convective heating, which provides the food with a more conventional appearance. It is found that the mushy zone can be completely eliminated for a suitable combination of conventional and microwave heating.

Marchant[16] models a material with an impurity that has a higher thermal absorptivity than the surrounding material. Experimentally it is found that hot spots occur at interfaces, such as two sections of a waveguide held together with glue. The glue has a higher thermal absorptivity than its surrounds and a hot spot is generated at the join. Thermal absorptivites of the form

$$\gamma(x,T) = \gamma_0 + (\gamma_1 + \gamma_2 T^{\gamma_3})\,\delta(x) \qquad (45)$$

are considered where $\delta(x)$ is the Dirac-delta function. This represents a material of constant thermal absorptivity with an additional source of temperature-dependent thermal absorptivity at the impurity. The forced heat equation (5) is considered incorporating the thermal absorptivity of equation (45) for a finite slab with fixed-temperature boundary conditions. Here the electric-field amplitude is assumed constant so that the theory is valid only for thin slabs, since the decay of the electric field is ignored.

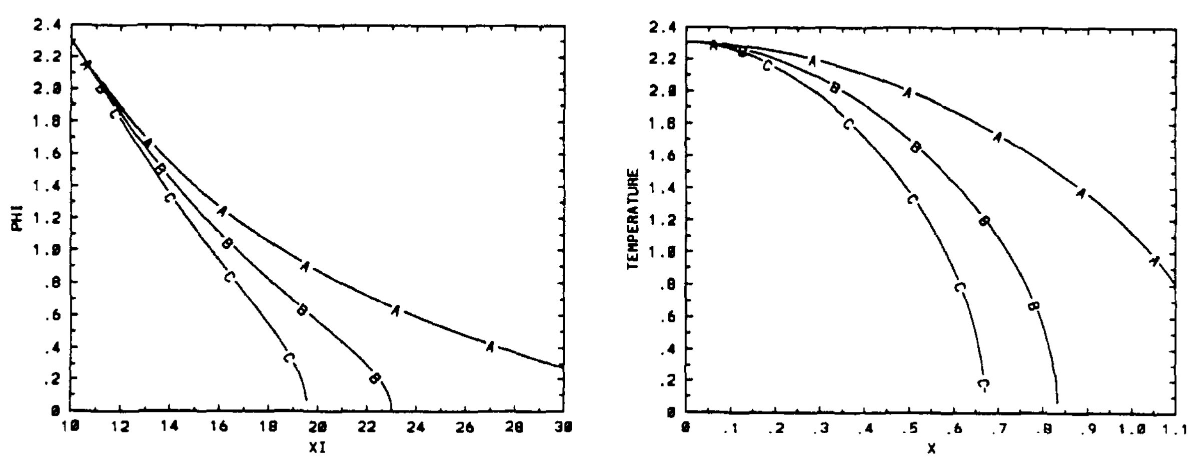

Figure 4. The solution (41a) for $m = 1$, $n = 3$, $\beta = 1$, and $t = 10$ and for $\alpha = 0.5$ (A), $\alpha = 1$ (B), and $\alpha = 2$ (C). *Figure 4a* shows the variable ϕ and *Figure 4b* shows the temperature T.

Steady-state temperature profiles are obtained and, for example, in the case $\gamma_3 = 2$ the profiles are

$$T = a_1 - \left(a_1 - \frac{\gamma_0}{2}\right)|x| - \frac{\gamma_0}{2}x^2$$
$$a_1 = \frac{1 \pm \sqrt{1 - \gamma_2(\gamma_0 + \gamma_1)}}{\gamma_2} \qquad \gamma_2(\gamma_0 + \gamma_1) < 1 \tag{46}$$

We notice that in this case there are again two steady-state temperature profiles in existence: the higher one is unstable while the lower one is stable. We notice also that the steady-state temperature profile only exists in a certain parameter range and outside this parameter range thermal runaway occurs.

The decay of the electric field as it propagates from the incident boundary and the interaction of the electric-field amplitude with temperature is also considered. For constant wavespeed, the thermal absorptivity must be proportional to the electrical conductivity so a balance is achieved between energy lost from the microwave radiation and heat absorption by the material. Assuming the electrical conductivity is proportional to the thermal absorptivity, equation (45) gives an electric-field amplitude of the form

$$|E| = e^{-\frac{\alpha}{2}[\gamma_0(x+1)+gu(x)]} \qquad g = \gamma_1 + \gamma_2 T^{\gamma_3}(0, t) \tag{47}$$

and $u(x)$ is the Heaviside step function. If no impurity is present in the material ($g = 0$), then the electric field decays exponentially with a decay rate of $\alpha\gamma_0/2$. With the impurity present, the electric-field amplitude is reduced by a factor of $e^{-\alpha g/2}$ at $x = 0$, and therefore the electric-field amplitude is reduced in the region $x > 0$ as the temperature increases. *Figure 5* shows stable steady-state temperature profiles of the forced heat equation (5) with electric-field amplitude (47). The thermal absorptivity is $\gamma = 5 + (2 + 1.8T)\delta(x)$ with $\alpha = 0.05$, 0.1, 0.2, and 0.4. As the decay rate α is increased, the heat absorption is lowered, which in turn lowers the steady-state temperature profiles. In addition, the temperature profiles become less nearly symmetric as the decay rate is increased. If the decay of the electric field is high enough, then the temperature peak occurs before the impurity (see the $\alpha = 0.4$ curve).

Kriegsmann et al.[2] consider a semi-infinite material with temperature-dependent electrical conductivity and thermal absorptivity, while the wavespeed of the system is assumed constant. This system is governed by Maxwell's equations (2) and the forced heat equation (5). The electrical conductivity and thermal absorptivity are assumed to have the form

$$\sigma = 2\gamma = \sigma_0 f\left(\frac{T}{T_i} - 1\right) \tag{48}$$

where f is an arbitrary function scaled so that $\sigma = \sigma_0$ at $T = T_i$. It is assumed that the temperature has reached a steady state and that the electric field comprises a steady-state amplitude and a time harmonic term,

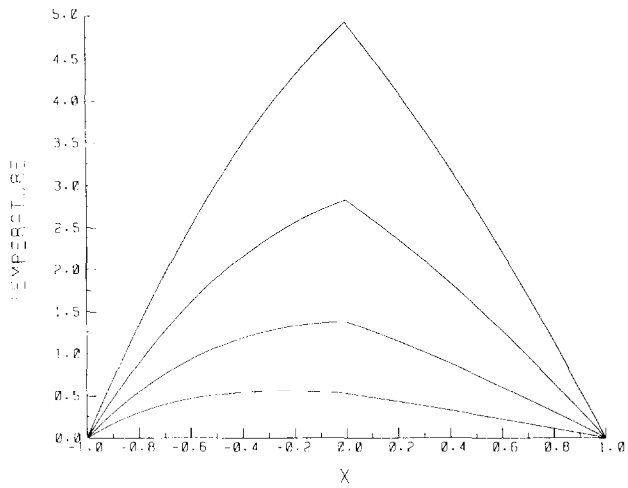

Figure 5. Stable steady-state temperature profiles of the forced heat equation (5) with electric-field amplitude (47). The thermal absorptivity is $\gamma = 5 + (2 + 1.8T)\delta(x)$ with $\alpha = 0.05$, 0.1, 0.2, and 0.4.

$$T = T(x) \qquad E = U(x)e^{-i\omega t} \tag{49}$$

Substituting equations (48) and (49) into (2) and (5) gives the coupled system

$$U_{xx} + Uk_1^2\left[1 + \frac{i\sigma_0}{\omega\epsilon}f\left(\frac{T}{T_i} - 1\right)\right] = 0$$
$$T_{xx} + \frac{\sigma_0}{2}f\left(\frac{T}{T_i} - 1\right)U^2 = 0 \tag{50a–b}$$

to solve for the electric-field amplitude U and the temperature T. The wave number in the material is $k_1 = k_v(\epsilon/\epsilon_v)^{-1/2}$, where ϵ_v is the electrical permittivity of free space. These equations are subject to the boundary condition

$$U_x + i\kappa_v U = 2i\kappa_v E_i \qquad x = 0 \tag{51}$$

which is equation (7) with the time harmonic component removed. The radiative and convective heat-loss boundary condition (9b) also applies. The authors assume that the electric conductivity is small ($\sigma_0 \ll 1$) and look for a perturbation solution,

$$U = U_0(x, X) + \sigma_0 U_1(x, X) + \dots$$
$$T = T_0(x, X) + \sigma_0 T_1(x, X) + \dots \tag{52}$$

using the method of multiple scales (the long length scale is $X = \sigma_0 x$). The form of the first-order solution is found for general electrical conductivity, $\sigma_0 f$, and the surface temperature (a measure of the heating of the slab) is found to be a monotonic increasing function of incident power. As the temperature increases, so does the electrical conductivity. This in turn reduces the electric-field amplitude in the material which limits the additional heating, a process the authors call "structural stabilization." This means that a steady-state temperature profile can be found for all choices of incident power.

Kriegsmann[19] considers a finite slab with the wavespeed assumed constant and the electrical conductivity and thermal absorptivity temperature dependent. The mathematical formulation of the problem is similar to Kreigsmann et al.,[2] with the addition of the boundary condition

$$U_x - ik_r U = 0 \text{ at } x = h \tag{53}$$

and equation (9c), which are the appropriate conditions for the electric-field amplitude and the temperature at the rear edge of the slab. In addition, the steady-state version of the forced heat equation is written in the form

$$T_{xx} + B_i p f\left(\frac{T}{T_i} - 1\right) U^2 = 0 \tag{54}$$

where p is an order one parameter which is the ratio of the power of an incident wave with amplitude unity to the power lost at the boundaries by convection. The steady-state solution is found as a series in the small Biot number ($B_i \to 0$), thus

$$\begin{aligned} T(x) &= T_0(x) + B_i T_1(x) + \dots \\ U(x) &= U_0(x) + B_i U_1(x) + \dots \end{aligned} \tag{55}$$

and where the ratio B_i/B_r is assumed fixed. The first-order solutions are obtained and these are used to determine the power as a function of the temperature in the slab. The conductivity is assumed to be monotonic increasing with temperature (in fact an exponential dependence on temperature is assumed). The power versus temperature curve is S-shaped, hence beyond a certain power level a large jump can occur in the steady-state temperature (and therefore a hot spot results). As the temperature stabilizes on the upper branch of the S-shaped curve, the sample is again structurally stabilized. A linear stability analysis is also performed, which shows that the steady-state temperature is stable when $dT/dp > 0$ and unstable when $dT/dp < 0$, with a hysteresis effect occuring.

Kriegsmann[20] formulates the problem as in Kriegsmann[19] obtaining the power versus temperature relationship

$$p = 2\frac{\left[(T - T_i) + \frac{B_r}{B_i}(T^4 - T_i^4)\right]}{\sigma(T)Q}$$

$$Q = \frac{1}{h}\int_0^h |U_0|^2 \, dx \tag{56}$$

by averaging the forced heat equation over the length of the slab. In equation (56), p is the ratio of the power generated by an electric field of amplitude unity to the power lost by conduction, T is the temperature, Q is the average of the square of the electric-field amplitude U_0 through the slab, and T_i is the ambient temperature. With the electrical conductivity $\sigma(T)$ chosen to have an exponential dependence on temperature, equation (56) exhibits the typical S-shaped response curve as described previously.

5. Damped wave equation model

Assuming that the electrical conductivity is small, and that the magnetic permeability and electrical permittivity are slowly varying functions of temperature, it is possible to reduce Maxwell's equation (2) to the damped wave equation (4). This equation, derived by Pincombe and Smyth,[3] describes the decay of the electrical field as it propagates through a medium with slowly varying properties and small conductivity. Pincombe and Smyth[3] consider equation (4) in conjunction with the forced heat equation (14) which is obtained by assuming that the time scale for heat absorption is much shorter than the time scale for heat diffusion ($\nu \ll \gamma$). Material properties of the form

$$\begin{aligned} &\sigma = \alpha\sigma' \qquad \gamma = \alpha\gamma' \qquad \alpha \ll 1, \\ &c = c_0(1 + c_1 T)^{c_2} \\ &\sigma' = \sigma_0(1 + \sigma_1 T)^{\sigma_2} \qquad \gamma' = \gamma_0(1 + \gamma_1 T)^{\gamma_2} \end{aligned} \tag{57}$$

are assumed where the small parameter α represents the magnitude of the electrical conductivity and of the slow variations. The perturbation solution is assumed to have the form

$$\begin{aligned} E &= a(X, \tau)e^{\frac{i\theta(X,\tau)}{\alpha}} + \alpha a_1(X, \tau)e^{\frac{i\theta(X,\tau)}{\alpha}} + \dots \\ T &= \alpha T_1(t, x, X, \tau) + \alpha^2 T_2(t, x, X, \tau) + \dots \end{aligned} \tag{58}$$

$$\tau = \alpha t \qquad X = \alpha x$$

This is a two-timing perturbation expansion, where the phase function θ represents the fast oscillations of the wave train, while the amplitude terms a and a_1 are modulated by slow variations only. Hence a and a_1 are functions of the new slow length and time scales X and τ, respectively. Notice also that the induced temperature is of order α. At order one substituting the expansion (58) into (4) and (14) gives

$$\theta_\tau + c\theta_X = 0 \qquad T_{1t} = \gamma'(\alpha T_1)a^2(X, \tau) \tag{59}$$

The first equation simply states that the wavetrain travels at speed c, while the second gives the heat absorption at order α. At order α in the expansion the transport equation,

$$a_\tau + ca_X = -\frac{1}{2}\left(\sigma' - c_X + \frac{c_\tau}{c}\right)a \tag{60}$$

is obtained, which governs the modulation of the first-order amplitude. Pincombe and Smyth[3] find explicit solutions to equation (60) for particular choices of equation (57) and compare them with numerical solutions of the damped wave equation (4) and the forced heat equation (14).

Smyth[5] considers a high-frequency radiation limit, which is also referred to as the geometrical optics limit and obtains the transport equation (60) directly from Maxwell's equations (2). This occurs because the assumption of high-frequency radiation is equivalent to the assumption of small electrical conductivity and slowly varying material properties, since in the high-frequency limit the wave train properties vary slowly over the scale of an extremely small wavelength. Smyth[5] assumes that the material properties depend linearly on temperature and are slowly varying, namely

$$\sigma = \sigma_0 + \alpha\sigma_1 T \qquad \mu = \mu_0 + \alpha\mu_1 T$$
$$\epsilon = \epsilon_0 + \alpha\epsilon_1 T \qquad \alpha \ll 1 \tag{61}$$

and develops perturbation solutions to the transport equation (60) and the forced heat equation (5) in the limit of small diffusivity. Using the method of strained co-ordinates solutions are found for semi-infinite, cylindrically symmetric, and spherically symmetric bodies. In addition a thermal boundary layer solution is developed for a fixed-temperature boundary condition and a zero heat-flux boundary condition. Smyth[21] considers the model first-order equation

$$E_t + c(T)E_x = -\sigma(T)E \tag{62}$$

which is essentially the transport equation (60) with a simplified form for the effective conductivity. Equation (62) is considered in conjunction with the forced heat equation (14). Power laws

$$c = c_0 T^{c_1} \qquad \sigma = \sigma_0 T^{\sigma_1} \qquad v = v_0 T^{v_1}$$
$$\gamma = \gamma_0 T^{\gamma_1} \tag{63}$$

are used for the material properties together with a solution method similar to that used in Smyth.[5] In this case the method of strained co-ordinates does not allow an explicit perturbation solution to be developed and the result is given in terms of an integral for which good agreement with numerical solutions is obtained.

Marchant and Pincombe[22] use the method of Smyth[5] to solve the damped wave equation (4) and the forced heat equation (5) in the limit of small diffusivity, with the power laws

$$\sigma = \alpha\sigma_0 \qquad \mu = 1 + \alpha\mu_1 T^{\mu_2} \qquad \epsilon = 1 + \alpha\epsilon_1 T^{\epsilon_2}$$
$$\gamma = \gamma_0 T^{\gamma_1} \qquad \alpha \ll 1 \tag{64}$$

taken for the material properties. As well as the method of strained co-ordinates, the method of multiple scales is introduced to enable an explicit solution to be obtained. The model includes the temperature dependency of the transmission and reflection of radiation at the boundary, with the electric-field amplitude at the boundary, to order α, given by

$$a(0,t) = 1 - \frac{\alpha\mu_1 c_v}{2(1+c_v)}(T^{\mu_2} - T_i^{\mu_2}) - \frac{\alpha\epsilon_1 c_v}{2(1+c_v)}(T^{\epsilon_2} - T_i^{\epsilon_2}) \tag{65}$$

where c_v is the wave speed of the radiation in free space and it is assumed that a wave of amplitude unity is transmitted at the initial temperature $T = T_i$. Hence it can be seen that the transmission of radiation decreases as the material heats up if the magnetic permeability and electrical permittivity are increasing functions of temperature. If the magnetic permeability and electrical permittivity are decreasing functions of temperature, then the reverse is true, with the transmission of radiation increased as the material heats up. *Figure 6a* shows the electric-field amplitude $|E|$ versus x for $\gamma = T^{1.17}$, $\sigma = 0.1$, $\mu = \epsilon = 1 + 0.1T^{-0.051}$, $\omega = 5$, $T_i = 1$, $\nu = 0$, $t = 5.6$ and a zero heat-flux boundary condition is applied. The figure shows the first-order asymptotic solution (——), the second-order asymptotic solution (-----), and the numerical solution (-·-·). *Figure 6a* shows the wavefront travelling more slowly at second-order, in addition the second-order asymptotic solution predicts a higher electric-field amplitude due to an increased transmission of radiation as the material heats up and to the effective conductivity (4b) being reduced at second order. These effects occur because the electrical permittivity and the magnetic permeability are both decreasing functions of temperature. *Figure 6b* shows the natural logarithm of temperature versus x for the same parameters as *Figure 6a*. The figure shows the first-order asymptotic solution (——), the second-order asymptotic solution (-----), and the numerical solution

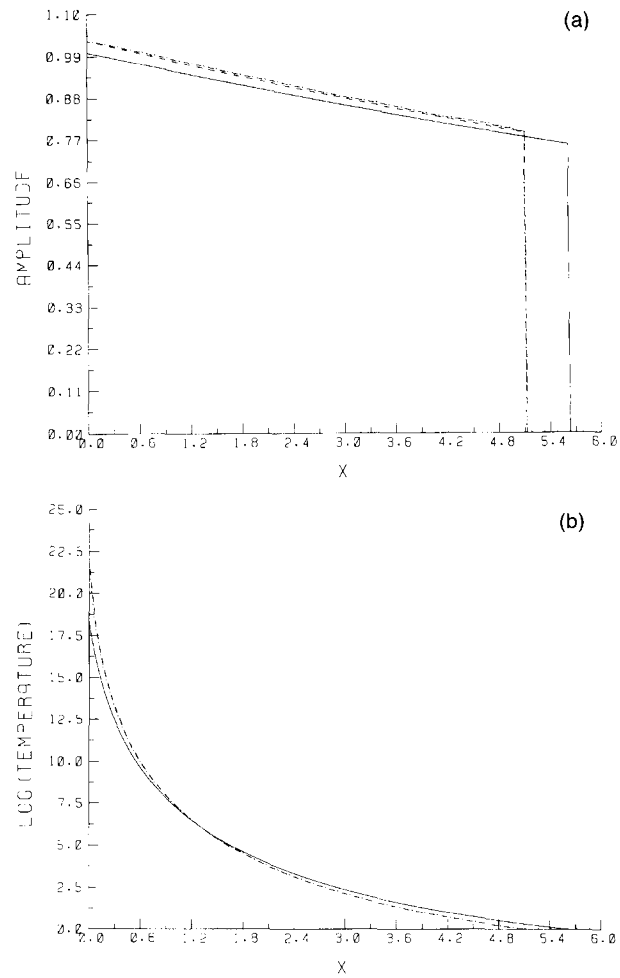

Figure 6. (a) The electric-field amplitude $|E|$ versus x for $\gamma = T^{1.17}$, $\sigma = 0.1$, $\mu = \epsilon = 1 + 0.1T^{-0.051}$, $\omega = 5$, $T_i = 1$, $\nu = 0$, $t = 5.6$ and a zero-heat flux boundary condition is applied. (b) The natural logarithm of temperature versus x for the same parameters as (a). Shown is the the first-order asymptotic solution (——), the second-order asymptotic solution (-----), and the numerical solution (-·-·).

(-·-·). In this case $\gamma_1 > 1$, so thermal runaway will occur at the boundary $x = 0$. The hot spot occurs at the boundary since the electric-field amplitude has a maximum there and there is no heat loss through the boundary. *Figure 6b* shows that the material is rapidly approaching thermal runaway at the boundary. Because the transmission of microwaves increases as the material heats up, the second-order theory predicts a higher temperature near the boundary and hence that thermal runaway will occur sooner than the first-order theory. Since the calculations and asymptotics are performed on the transformed variable, $\theta = T^{1-\gamma_1}$, which remains bounded, there is an extremely good correspondence between the numerical solution and the second-order asymptotic solution even just before thermal runaway occurs (see *Figure 6b* near $x = 0$).

Pincombe and Smyth[23] consider the damped wave equation (4) and the forced heat equation (14) assuming power laws of the form

$$p = p_1 + \alpha p_2 T^{p_3} \qquad \alpha \ll 1 \tag{66}$$

for all material properties. A semi-infinite slab is considered with a zero heat-flux boundary condition and includes the temperature-dependent transmission of radiation (see equation [65]). Using the methods of characteristics and multiple scales, perturbation solutions are developed for the case of small thermal absorptivity. These perturbation solutions are compared with numerical solutions of (4) and (5).

Marchant and Smyth[6] consider a material that has non-Ohmic electrical conductivity and thermal absorptivity with constant wavespeed,

$$\begin{aligned} \sigma(E, T) &= (\sigma_0 + \sigma_1 T^n)(1 + \alpha_1 E) \\ \gamma(E, T) &= (\gamma_0 + \gamma_1 T^n)(1 + \beta_1 E) \end{aligned} \tag{67}$$

and show that the propagation of microwaves is governed by a modified damped wave equation

$$E_{tt} + (\sigma E)_t = c^2 E_{xx} \tag{68}$$

and the forced heat equation (5) with thermal absorptivity and electrical conductivity given by equations (67). Notice that the dependence of equations (6) on the electric field and the temperature couples (5) and (68). A perturbation solution is found for small electrical conductivity, and a full numerical solution is developed using the method of characteristics. In addition, a Ginzburg-Landau equation is derived for $a = |E|$ assuming small amplitude and slowly varying scales,

$$ia_\tau - a_{\zeta\zeta} + (a_1 + ia_2)|a|^2 a = 0 \tag{69}$$

where τ is a slow time scale, ζ is a slow scale moving at the characteristic speed, and a_1 and a_2 are constants. In general the Ginszburg-Landau equation posesses breather, hole and front solutions. Due to the particular form of equation (69), these exact solutions do not exist in this case; however, asymptotic solutions such as a slowly varying soliton and a moving front solution are found. *Figure 7* shows a slowly varying soliton which is a solution of equation (69). The figure shows the asymptotic theory (——) for both $t = 0$ and $t = 10$, which is compared with the numerical solution at $t = 10$. The soliton moves slowly to the right as it decays and good agreement is obtained between the numerical solution and the asymptotic theory.

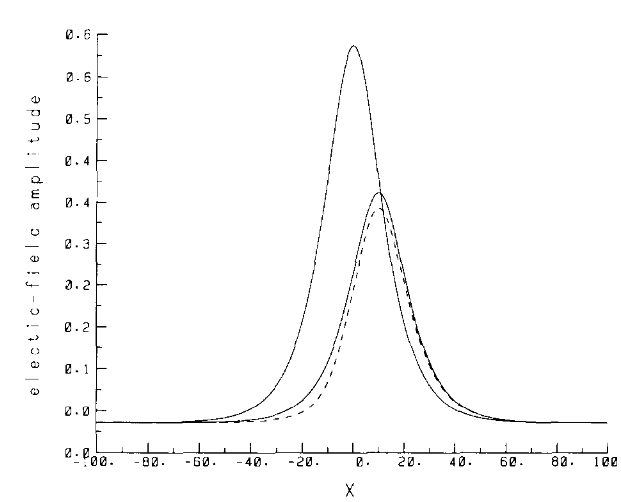

Figure 7. A slowly varying soliton which is a solution of equation (69) is shown. Drawn is the asymptotic theory (——) for both $t = 0$ and $t = 10$ and the numerical solution for $t = 10$.

6. Dynamics and control of thermal runaway

Kriegsmann[4] considers the steady-state model of Kriegsmann[19] with the steady-state version of the forced heat equation (54) replaced by the full forced heat equation

$$T_t = T_{xx} + B_i pf\left(\frac{T}{T_i} - 1\right)U^2 \tag{70}$$

to enable the dynamical behavior of the heating process to be modelled. Equations (70) and (50a) are solved in the small Biot number limit ($B_i \ll 1$), subject to boundary and initial conditions (50), (52) and (9), by the method of multiple scales,

$$\begin{aligned} T &= T_0(\tau) + B_i T_1(x, \tau) + \dots \\ U &= U_0(x, \tau) + B_i U_1(x, \tau) + \dots \end{aligned} \tag{71}$$

The slow time scale, $\tau = B_i t$, is introduced since the forcing term in (70) is order B_i, hence the temperature and the electric-field amplitude are modified on this slow time scale. Notice that because the heating is order B_i and the slab is nearly insulated the order one temperature is spatially uniform.

At first-order the evolution equation

$$\frac{\partial T_0}{\partial \tau} = -2\left[T_0 - T_i + \frac{B_r}{B_i}(T_0^4 - T_i^4)\right] + pf\left(\frac{T_0}{T_i} - 1\right)\gamma \qquad \gamma = \frac{1}{h}\int_0^h U_0^2 \, dx \tag{72}$$

is obtained for the first-order temperature in the slab. In the steady state, $\partial T_0/\partial \tau = 0$ (72) becomes the power versus temperature relation (56). A procedure for controlled heating is analyzed with the power changing on the slow time scale,

$$p(\tau) = p_1 + (p_0 - p_1)e^{-\lambda(\tau-\tau_0)} \qquad \tau > \tau_0 \tag{73}$$

To speed up the heating of the sample, a power level p_0 is used initially, which without modification would lead to thermal runaway. At time $\tau = \tau_0$, the power is decreased exponentially such that the power level approaches p_1 as $\tau \to \infty$, where if the power level p_1 where applied initially it would result in a steady-state temperature on the lower branch of the S-shaped curve. It is found that there is a critical temperature above which the material experiences a thermal runaway and below which the temperature evolves to the lower branch of the S-shaped curve.

Kriegsmann[24] considers a simple control model for microwave heating by averaging the forced heat equation over the length of a thin slab to obtain

$$\frac{dT_0}{dt} = -2[B_i(T_0 - T_i) + B_r(T_0^4 - T_i^4)] + \frac{\sigma(T_0)}{2}p \tag{74}$$

where T_0 is the leading-order temperature in the small Biot number limit and p is the microwave power density. Note that the electric-field amplitude is assumed constant because the slab is thin and the power is assumed to depend on the temperature through the relation

$$\frac{dp}{dt} = -\gamma(p - p_s) - \beta(T_0 - T_s) \tag{75}$$

where the parameters γ and β are positive. Relation (75) provides feedback to the heating process to stabilize it at the desired steady-state, at which the temperature is T_s and the power is p_s. It is assumed that the electrical conductivity obeys the Arrhenius law

$$\sigma(t) = \sigma_A + \sigma_B e^{-x/(T-T_A)} \tag{76}$$

Hence the power versus temperature curve has the usual S-shaped profile even though a thin slab is considered. It is found that for the appropriate choice of γ and β, that the system, for any initial power level, will evolve to a steady state on the upper branch on the S-shaped curve without ever exceeding the melting point of the material. Inappropriate choices of the feedback parameters lead to overshoot, where the material is heated beyond its melting point, and thus destroyed, or lead to relaxation oscillations where the system never reaches a steady state.

Kriegsmann[25] considers the control process of Kriegsmann[24] for a thin cylindrical sample. The cylinder has length L and radius d, with the ratio d/L assumed small. The leading-order temperature satisfies

$$T_t = T_{zz} - 2[B_i(T - T_i) + B_r(T^4 - T_i^4)] + \frac{\sigma(T)}{2}|E(z)|^2 \tag{77}$$

with zero heat-flux boundary conditions applied at the ends of the rod $z = 0, h$. Depending on the type of incident electromagnetic mode used to heat the material, the electric-field amplitude can vary along the length of the rod. In particular a maximum in amplitude can occur in the middle of the rod which leads to raised temperatures at this location. This form of heating is potentially useful for joining applications.

7. Numerical modelling

Jolly and Turner[26] apply Maxwell's equations (2) with zero electrical conductivity and constant magnetic permeability and the forced heat equation (5) to a one-dimensional slab. At the front edge of the slab a convective heat-loss boundary condition is applied ([9b] with $B_r = 0$) while at the rear edge of the slab a zero heat-flux boundary condition is applied ([9c] with $B_i = B_r = 0$). The solution is assumed time harmonic so the boundary conditions for the electric field are (51) and (53) with $k_c = 0$. These allow reflection and transmission of radiation at the front edge and complete reflection of radiation at the rear edge of the slab. The equations are solved numerically using a finite-difference scheme with the absorbed power and temperature profiles showing peaks and troughs. This is due to the standing wave pattern set up by the incident and reflected electric fields. The authors examine the effect of extending the slab using a loss-less material such as teflon. This alters the standing wave pattern in the material and can result in flatter power and temperature profiles. The electrical permittivity and thermal absorptivity are assumed to have a cubic dependence on temperature.

Turner and Jolly[27,28] examine the application of microwave energy in drying porous materials such as wood or bricks. The model of Jolly and Turner[26] is extended to examine the mass and heat transfer which occurs during the combined microwave and convective drying of a porous material. The material consists of a solid matrix, in which a liquid phase and a gaseous phase where both air and water vapor reside. The equations that govern the drying process are conservation of mass, liquid, and enthalpy coupled with the appropriate flux laws (Darcy's for the gas and liquid, Fick's for the water vapor). The boundary conditions adopted allow convective drying at the front edge of the slab while the rear edge of the slab is impermeable. These equations are considered in conjuction with the form of Maxwell's equations and the forced heat equation considered by Jolly and Turner.[26] In this case the electrical permittivity and the thermal absorptivity are both moisture- and temperature-dependent. This is due to the fact the energy absorption is high when a large water fraction is present in the material. The results show that the combined use of convective and microwave drying can halve drying times. The microwave radiation heats the moisture deep within the material, causing the moisture to be pumped to the surface. When the material is nearly dry, care must be taken to avoid thermal runaway and thus damage to the sample. The authors present perspective plots of power absorption over time for combined microwave and convective drying of a brick. These show that peaks in power absorption occur which are due to the standing waves set-up in the brick arising because reflection occurs from the metal backing.

DoRego et al.[29] consider the microwave joining of polymers, which requires the material to be joined (in this example Nylon-6) to be placed in a ridged wave guide, which concentrates the microwave energy at the weld. As the thermal absorptivity of Nylon-6 is temperature-dependent, thermal runaway can occur, destroying the sample. A two-dimensional finite-difference model is developed to predict the occurence of thermal runaway. The appropriate version of the forced heat equation (5) is considered subject to convective heat-loss boundary conditions ([9] with $B_r = 0$) on the slab's boundaries. The form of the thermal absorptivity $\gamma(T)$, is found from the tabulated dielectric loss data available for Nylon-6 over the temperature range of interest. The incident electric-field amplitude, determined from ridged waveguide theory, is assumed constant over the area of the join and zero elsewhere on the slab. The model predicts the temperature distribution over the slab for a given incident power and exposure time. For an effective join, the maximum temperature needs to be greater than the melting point but less than the temperature at which combustion occurs so the material is not destroyed.

Pincombe and Smyth[3] and Marchant and Pincombe[22] develop a numerical solution of the damped wave equation (4) and the forced heat equation (5) for a semi-infinite slab subject to initial and boundary conditions (7) for the electric field, which allow reflection and transmission of the incident electric field and zero heat-flux and fixed-temperature boundary conditions. The damped wave equation is discretized using a three-point centered difference scheme in space and a four-point centered scheme in time, while for the forced heat equation a variant of the Crank-Nicolson finite-difference scheme is used. If the numerical scheme discretized the electric field over the discontinuity at the wavefront, then unphysical oscillations appear in the solution due to the large x-derivatives at the wavefront. To overcome this the spatial discretization is carried out up to the wavefront where the exact value is known for the electric field. This enables the position of the wavefront and the electric field in the region of the wavefront to be accurately determined.

References

1. Portis, A. M. *Electromagnetic Fields: Sources and Media.* John Wiley & Sons, 1978
2. Kriegsmann, G. A., Brodwin, M. E. and Watters, D. G. Microwave heating of a ceramic halfspace. *SIAM J. Appl. Math.* 1990, **50**, 1088–1098
3. Pincombe, A. H. and Smyth, N. F. Microwave heating of materials with low conductivity. *Proc. Roy. Soc. Lond. A* 1991, **433**, 479–498
4. Kriegsmann, G. A. Thermal runaway in microwave heated ceramics: A one-dimensional model. *J. Appl. Phys.* 1992, **71**, 1960–1966
5. Smyth, N. F. Microwave heating of bodies with temperature dependent properties. *Wave Motion* 1990, **12**, 171–186
6. Marchant, T. R. and Smyth, N. F. Microwave heating of materials with non-Ohmic conductance. *SIAM J. Appl. Math.* 1993, **53**, 1591–1612
7. Metaxas, A. S. and Meredith, R. J. *Industrial Microwave Heating.* IEE Power Engineering Series 4, P. Peregrinus, London, 1983
8. Hill, J. M. Simple exact solutions applicable to microwave heating. *J. Appl. Math. Phys. (ZAMP)* 1990, **40**, 872–882
9. Hill, J. M. and Jennings, M. J. Formulation of model equations for heating by microwave radiation. *Appl. Math. Model.* 1993, **17**, 369–379
10. Von Hippel, A. R. *Dielectric Materials and Applications.* MIT Press, Cambridge, MA, 1954
11. Coleman, C. J. On the microwave hotspot problem. *J. Aust. Math. Soc. Ser. B* 1991, **33**, 1–8
12. Hill, J. M. and Smyth, N. F. On the mathematical analysis of hotspots arising from microwave heating. *Math. Eng. Industry* 1990, **2**, 267–278
13. Roussy, G., Bennani, A. and Thiebaut, J. Temperature runaway of microwave irradiated materials. *J. Appl. Phys.* 1987, **62**, 1167–1170
14. Brodwin, M. E. Kriegsmann, G. A. and Watters, D. G. Temperature instability in the microwave heating of a uniformly illuminated planar slab. *IEEE*, 1995, in press
15. Hill, J. M. and Pincombe, A. H. Some similarity temperature profiles for the microwave heating of a half-space. *J. Aust. Math. Soc. Ser. B* 1991, **33**, 290–320
16. Smyth, N. F. The effect of conductivity on hot-spots. *J. Aust. Math. Soc.* B 1992, **33**, 403–413
17. Coleman, C. J. Microwave heating of frozen substances. *Appl. Math. Model.* 1990, **14**, 439–443
18. Marchant, T. R. Microwave heating of materials with impurities. *J. Eng. Math.* 1994, **28**, 379–400
19. Kriegsmann, G. A. Microwave heating of ceramics. *Ordinary and Partial Differential Equations 3*, ed. B. Sleeman and R. Jarvis, Longman House, 1991, pp. 45–56
20. Kriegsmann, G. A. Microwave heating of ceramics: A mathematical theory. *Microwaves: Theory and Applications in Materials Processing*, ed. D. E. Clarke, F. D. Gac, and W. H. Sutton, Ceramic Transactions 21, American Ceramic Society, 1991, pp. 117–183
21. Smyth, N. F. A model of microwave heating. Research report, Department of Mathematics, University of Edinburgh, 1992
22. Marchant, T. R. and Pincombe, A. H. Microwave heating of materials with temperature, dependent wavespeed. *Wave Motion* 1994, **19**, 67–82
23. Pincombe A. H. and Smyth N. F. Microwave heating of materials with power law temperature dependencies. *IMA J. Appl. Math.* 1994, **52**, 141–176
24. Kriegsmann, G. A. Feedback stabilization of thermal runaway in microwave heated ceramics. *J. Am. Ceramic Soc.* 1995, submitted
25. Kriegsmann, G. A. Thermal runaway and its control in microwave heated ceramics. *Mat. Res. Soc. Symp. Proc.* 1992, **269**, 257–264
26. Jolly, P. G. and Turner, I. W. Non-linear field solutions of one-dimensional microwave heating. *J. Microwave Power Electromag. Energy* 1990, **25**, 3–15
27. Turner, I. W. and Jolly, P. G. The effect of dielectric properties on microwave drying kinetics. *J. Microwave Power Electromag. Energy* 1990, **25**, 211–223
28. Turner, I. W. and Jolly, P. G. Combined microwave and convective drying of a porous material. *Drying Technol.* 1991, **9**, 1209–1269
29. DoRego D., Cooper P., Siores E. and Marchant T. R. Two-dimensional transient heat transfer computations of microwave joining of polymers. In FABCON/FABFAIR, Towards a Competitive Edge. *Conference Proceedings Welding Technology Institute of Australia*, Wollongong 1993